Ceramics International 44 (2018) 18491–18498

Contents lists available at ScienceDirect

Ceramics International

journal homepage: www.elsevier.com/locate/ceramint

Dielectric relaxation and phase transition behavior of $(1–x)Pb(Zn_{1/3}Nb_{2/3})O_3$-$xBaTiO_3$ binary solid solutions

Qiang Gao[a], Qingyuan Hu[a,*], Li Jin[a], M.V. Gorev[b,c], D.S. Chezganov[e], E.O. Vlasov[e], Huarong Zeng[d], Luyang Zhao[a], Yu Cui[a], Zhuo Xu[a], Xiaoyong Wei[a,*]

[a] Electronic Materials Research Laboratory, Key Laboratory of the Ministry of Education & International Center for Dielectric Research, School of Electronic and In formation Engineering, Xi'an Jiaotong University, Xi'an 710049, China
[b] Kirensky Institute of Physics, Federal Research Center KSC SB RAS, Krasnoyarsk 660036, Russia
[c] Institute of Engineering Physics and Radio Electronics, Siberian Federal University, Krasnoyarsk 660041, Russia
[d] State Key Laboratory of High Performance Ceramics and Superfine Microstructures, Shanghai Institute of Ceramics, Chinese Academy of Sciences, Shanghai 200050, China
[e] School of Natural Sciences and Mathematics, Ural Federal University, Ekaterinburg 620000, Russia

ARTICLE INFO

Keywords:
Dielectric relaxation
Phase transition
"U"-shaped variation
Polarization mismatch

ABSTRACT

Dielectric relaxation and phase transition behaviors in $(1–x)Pb(Zn_{1/3}Nb_{2/3})O_3$-$xBaTiO_3$ (PZN-BT) binary solid solutions have been systematically studied in this paper. All the compositions display a pure pseudo-cubic perovskite structure. As the BT contents increase from 10 mol% to 70 mol%, the phase transition peak becomes broader and broader, accompanying with decreases of ε_m (the maximum dielectric permittivity) and T_m (the temperature corresponds to the ε_m). Nevertheless, an abnormal increase of ε_m and T_m occurs when the BT contents exceeds 70 mol%, forming a "U" shaped curve of the compositional dependence of ε_m and T_m. Moreover, it is indicated from the new glass model fitting results that the characteristic parameter p, which represents the degree of relaxation, also shows a similar "U" shaped variation curve. Similarly, as shown in polarization-electric field loops, both remnant polarizations (P_r) and coercive fields (E_c) display the "U" shaped curve as the BT content changes from 10 mol% to 80 mol%. Finally, according to the similar variation of these key parameters mentioned above, a polarization mismatched model, which describes the destruction and reestablishment of the long range order arrangement in solid solutions composed of two kinds of ferroelectrics, is proposed to illustrate the underlying mechanism. In this PZN-BT system or other similar ABO_3-type perovskite relaxors, the competition between the A-O and B-O coupling plays an important role to form the "U" shaped evolution of these key parameters.

1. Introduction

Relaxor ferroelectrics always exhibit outstanding electrical properties and have been extensively studied since their advent in 1950s [1–4]. Moreover, some of them with superior performances have been technically applied in a variety of industrial areas including energy storage capacitors, piezoelectric actuators, electrostrictive devices, and so on [5–9]. Physics underlying the relaxor ferroelectrics has long been a controversial topic in the study of ferroelectric materials. Generally, the characteristics which distinguish the relaxor ferroelectrics from normal ferroelectrics are the diffusive phase transition (DFT) and frequency dispersion. Many different theories have been proposed to explain the special dielectric property of the relaxor ferroelectrics, such as local compositional fluctuation, micro-macro domain, random field, and so on [10–13]. As the developing of high resolution structural analysis methods, polar nano regions are observed and generally accepted as the structural origin of the excellent electrical performance of relaxor ferroelectrics [14–16].

Typical $AB'B''O_3$ type relaxor ferroelectrics, like PMN and PSN, have two different kinds of ions at the B-site of the perovskite structure [17,18]. Thus, the B-site long range order structure is destructed due to the different valences and ionic radius between B-site ions, resulting in the formation of polar nano regions [19]. With the developing of research, many novel relaxor ferroelectric solid solutions are discovered, and their constitution can be described as $A'A''B'B''O_3$. Thus, both the A and B-site long range order structure are destructed simultaneously, leading to a stronger relaxation which means that the diffusive phase transition takes place in a broader temperature range. These materials

* Corresponding authors.
E-mail addresses: huqingyuan0408@mail.xjtu.edu.cn (Q. Hu), wdy@mail.xjtu.edu.cn (X. Wei).

https://doi.org/10.1016/j.ceramint.2018.07.069
Received 9 May 2018; Received in revised form 6 July 2018; Accepted 8 July 2018
Available online 09 July 2018

also have shown great potential in temperature stable dielectric and energy storage capacitors [20–22].

Among the $A'A''B'B''O_3$ relaxor ferroelectrics, one class with special dielectric behavior is focused here. In this kind of relaxor ferroelectric, the compositional dependence of the Curie point (T_C) changes in a "U"-shaped curve. Reported solid solutions with such a unique behavior include $BaTiO_3$-$Bi(Mg,Ti)O_3$, $BaTiO_3$-$BiFeO_3$ and $BaTiO_3$-$Pb(Mg_{1/3}Nb_{2/3})O_3$ [23–25]. Generally, T_C is the temperature at which the long range order structure disappears. When the A and B- site of the perovskite structure are occupied by two or more different kinds of ions, the long range order area shrinks, which results in a lower T_C. However, the "U"-shaped variation of T_C in these special systems has not been discussed thoroughly.

In addition, it worth noting that these relaxor ferroelectrics are generally solid solutions of two different ferroelectrics or one ferroelectric and one relaxor ferroelectric. Hence that, the $Pb(Zn_{1/3}Nb_{2/3})O_3$-$BaTiO_3$ solid solution is also expected to show a similar dielectric behavior. $Pb(Zn_{1/3}Nb_{2/3})O_3$ is a typical relaxor ferroelectric with rhombohedral perovskite structure at room temperature [26,27]. Single perovskite structure can also be obtained in PZN-based solid solutions, such as $Pb(Zn_{1/3}Nb_{2/3})O_3$-$BaTiO_3$ (PZN-BT), $Pb(Zn_{1/3}Nb_{2/3})O_3$-$SrTiO_3$ (PZN-ST), and $Pb(Zn_{1/3}Nb_{2/3})O_3$-$PbTiO_3$ (PZN-PT), and so on. BT, PT and ST in these solid solutions are used to stabilize the phase structure. Among these additives, BT is the most effective one to suppress the formation of the pyrochlore phase [28–30]. It is also reported that the PZN-BT system shows strong DPT behaviors [31]. Nevertheless, compositional dependence of the phase structure and dielectric property has not been reported in the (1 − x)PZN-xBT system.

In this work, we performed detailed investigation on the compositional dependence of phase transition and polarization behaviors in the PZN-BT system. On basis of the obtained results, we proposed a polarization mismatched model to explain the evolution of the relaxor and ferroelectric state in the PZN-BT system.

2. Experimental procedure

The compositions selected for this study were $(1–x)Pb(Zn_{1/3}Nb_{2/3})O_3$-$xBaTiO_3$ (x = 0.1–0.8). PbO (99.9%), ZnO (99.9%), Nb_2O_5 (99.9%), TiO_2 (99.9%) and $BaCO_3$ (99.9%) were used as starting raw materials (Sinopharm Chemical Reagent Co. Ltd, Shanghai, China). Ceramics were prepared by means of a two-step columbite reaction method. Firstly, ZnO and Nb_2O_5 mixed in 1:1 stoichiometric ratio were ball-milled for 12 h. After drying, the mixtures were calcined at 1000 °C for 6 h. Then, the precursor was mixed with PbO, TiO_2 and $BaCO_3$ in stoichiometric ratio and milled for 12 h. After drying, the powders were pre-sintered at 900 °C for 2 h in a sealed Al_2O_3 crucible. The pre-sintered powders were ball milled again and dried. The dried powders were well mixed with a 5 wt% PVA binder, pressed into 12 mm in diameter and 1 mm in thickness pellets under a pressure of 150 MPa. The binder was burnt out at 600 °C for 2 h in air. Finally, the samples were sintered at temperature range from 1190 °C to 1350 °C in a sealed Al_2O_3 crucible in case PbO evaporation from the pellets.

Phase structure of the ceramics samples was examined by X-ray diffractometer (XRD, Rigaku D/Max-2400, Tokyo, Japan) using CuKα radiation (λ = 0.15406 nm) operating at 40 kV and 100 mA. The microstructures of the ceramics samples were observed by using scanning electron microscopy (SEM, FEI Quanta 250 FEG, Hillsboro, OR, USA). Temperature-dependent dielectric spectra were measured by a LCR meter (Agilent HP4284A, Santa Clara, CA, USA) with a frequency range from 100 Hz to 100 kHz. Ferroelectric polarization-electric field (*P-E*) hysteresis loops were measured at 1 Hz using a ferroelectric test system (TF Analyzer 2000E, aixACCT, Aachen, Germany). The linear thermal expansion has been measured in the temperature range 100–650 K using the induction pushrod dilatometer Netzsch DIL-402C calibrated with a silica glass as a standard. Measurements were performed in a dynamical mode with heating and cooling rates of 2–3 °C/min in a flow of dry helium (O_2 concentration is about 0.05% of volume). The sample loading was 30 cN.

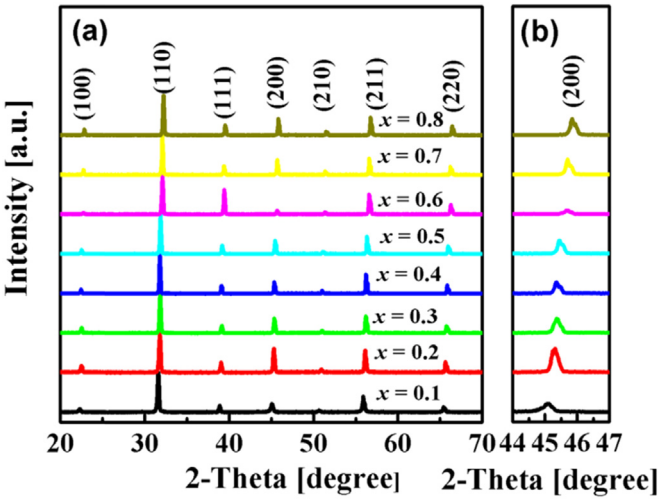

Fig. 1. (a) XRD patterns of (1 −x)PZN-xBT (x = 0.1–0.8) ceramic samples with a scanning angle from 20° to 70°. (b) Enlarged XRD patterns from 45.0° to 46.0° of (1 − x)PZN-xBT ceramics.

3. Results and discussion

XRD patterns of the $(1–x)$PZN-xBT (x = 0.1–0.8) with a scanning angle from 20° to 70° are shown in Fig. 1(a). Pure perovskite structure without any detectable pyrochlore phase can be seen in the XRD patterns. In addition, no splitting of the (200) peak, corresponding to a tetragonal symmetry, can be observed in Fig. 1(b). Therefore, the phase structure should be pseudo-cubic perovskite structure. With the increasing BT contents, diffraction peaks gradually shift toward higher degree, indicating that the inter-planar spacing becomes wider and wider.

Fig. 2 shows the SEM micrographs from the thermally etched surface of PZN-BT ceramics. The etching condition is generally 200 °C lower than the sintering temperature and for 15 mins. It is found that the samples exhibit dense microstructure and clear grain boundaries. With the increasing BT contents, the average grain size decreases obviously.

Fig. 3 shows the temperature dependence of the dielectric constant (ε'(T)) and loss tangent (tanδ(T)) measured at 0.1, 1, 10, 50 and 100 kHz, respectively. It can be seen that all the PZN-BT compositions exhibit obvious DPT. Meanwhile, the frequency dispersions in ε'(T) and tanδ(T) are also observed, indicating the dielectric relaxation behaviors in this system. Temperature dependence of ε' (at 1 kHz) for compositions with x = 0.2–0.8 is shown in Fig. 4(a). For compositions with $0.5 \le x \le 0.7$, dielectric peaks are relatively broader. Correspondingly, the maximum permittivity (ε_m) and T_m (at which the ε_{max} is observed) are also smaller. Fig. 4(b) shows the T_m and ε_m as a function of BT contents in the $(1–x)$PZN-xBT system. T_m firstly decreases from 140 °C at x = 0 to − 117 °C at x = 0.7, and then increases from − 117 °C at x = 0.7–120 °C at x = 1.0. In another way, T_m changes in the form of a "U" shaped curve. Generally, the dielectric relaxation behavior caused by the addition of PZN in BT ceramics can be explained in terms of the assumption proposed by Bokov et al. [14] According to their assumption, a large difference in valence between B′ and B″ ions and small size of A-site cation would increase the elastic drive toward ordering on B-site in $A(B'B'')O_3$ system, and the DPT becomes sharper by increasing the B-site cation ordering. In this work, Pb^{2+} ion radii is smaller than that of Ba^{2+} ion at the A-site, whereas both Zn^{2+} and Nb^{5+} ions radius are smaller than that of Ti^{4+} ion at the B-site, resulting in the observed

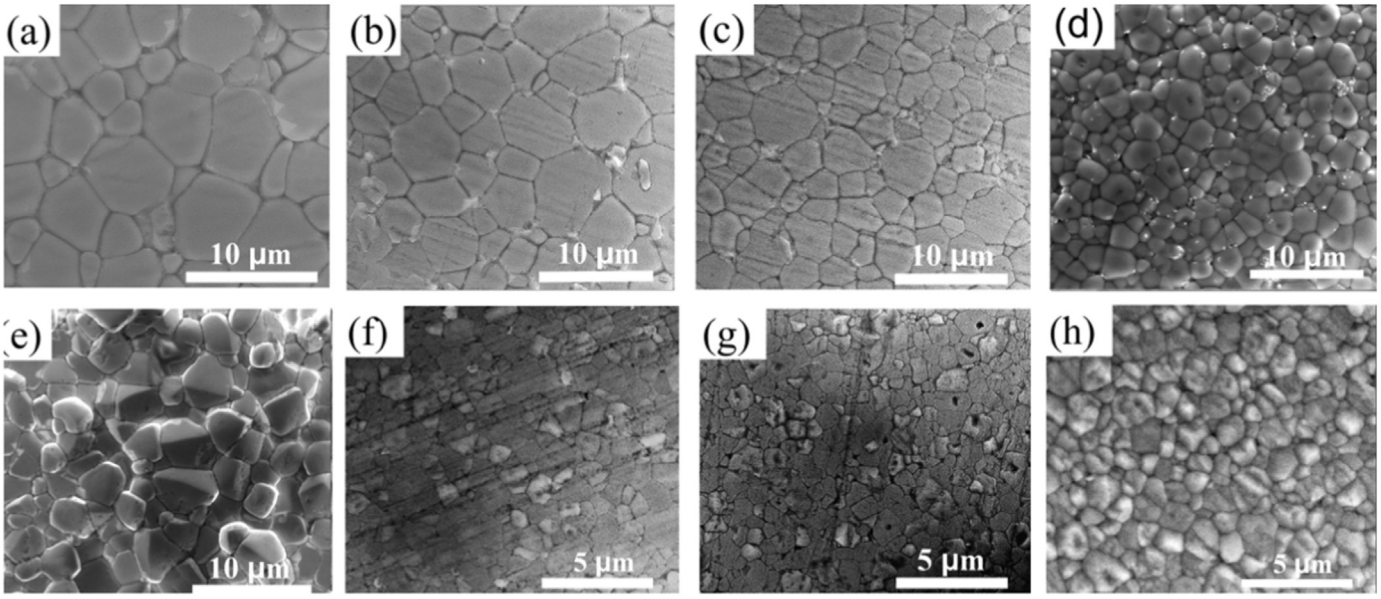

Fig. 2. SEM images of thermally etched surfaces of the $(1-x)$PZN-xBT ceramics sample with $x = 0.1$–0.8, corresponding to (a)–(h). Thermal etching was performed at 100 °C below the sintering temperature of PZN-BT ceramics for 30 min.

relaxation behavior.

For relaxor ferroelectrics, the relaxor nature is usually analyzed by a modified Curie-Weiss law [32,33], which can be written as:

$$\frac{1}{\varepsilon} - \frac{1}{\varepsilon_m} = \frac{(T - T_m)^\gamma}{C}, \tag{1}$$

where ε_m is the maximum value of the dielectric permittivity, T_m is the temperature corresponding to the ε_m, C is the Curie-like constant, and γ is the degree of diffuseness. For $\gamma = 1$, Eq. (1) is equivalent to the Curie-Weiss law, indicating a normal ferroelectric. The fitting results by Eq. (1) are shown in Fig. 5. Values of γ for $(1-x)$PZN-xBT ($x = 0.1$–0.8) are shown in Table 1. The γ value shows a small variation from 1.64 to 1.83, indicating that these compositions exhibit similar relaxation degree. To further characterize the variation of relaxation degree in this PZN-BT system, the new glass model is also used and can be described as [34] (Fig. 6).

$$\omega = \omega_0 \exp\left[-\left(\frac{T_0}{T_m}\right)^p\right], \tag{2}$$

where T_0 is the ratio of the activation energy to the Boltzmann constant κ_B, T_m is the temperature corresponding to the ε_m, ω_0 is the characteristic frequency, which is equal to $2\pi f$. The value of parameter p can be used to describe the dielectric relaxation strength (DRS) and relation among normal ferroelectrics, relaxor ferroelectrics, the Debye medium and glass. For relaxor ferroelectrics, p is always larger than 1, and increases with the decreasing DRS. Logarithm of frequency (Inω) as a function of reciprocal of temperature ($1/T$) and the fitting results by Eq. (2) are shown in Fig. 7(a). All of the data show excellent fittings ($R^2 > 0.998$ for all compositions). Fitting parameters p, E_a and ω_0 obtained from the fitting to the new glass model are summarized in Table 2. It should be noted that all the parameters obtained for $x = 0.3$ compositions are anomalous and unreasonable, although repeated experiments were performed. Generally, the activation energy E_a decreases with the increasing BT concentration. E_a of studied compositions are higher than that of 0.9PMN-0.1PT relaxor ferroelectrics (E_a–0.046 eV) [35] and smaller than that of $BaTiO_3$-$BiSnO_3$ (E_a–0.25 eV) [19]. It is clear that the addition of PZN induces a shift toward relaxor ferroelectrics on basis of the physical meaning of p. This phenomenon is also in accordance with reports in other relaxor systems [24,36].

ΔT_m, which is used to characterize the degree of frequency dispersion in the frequency range from 100 Hz to 100 kHz, is defined as follows [37]:

$$\Delta T_m = T_{m(100\ \mathrm{kHz})} - T_{m(100\ \mathrm{Hz})} \tag{3}$$

where $T_{m\ (100\mathrm{kHz})}$ and $T_{m\ (100\mathrm{Hz})}$ are the temperature of dielectric peak measured at 100 kHz and 100 Hz, respectively. Values of p and ΔT_m as a function of BT contents are shown in Fig. 7(a) and (b). It is indicated that ΔT_m changes in a similar way as that of parameter p. Thus, the new glass model characterizes relaxor behavior of the PZN-BT system properly.

Temperature dependence of thermal expansion coefficient (α) and strain ($\Delta L/L$), for samples with $x = 0.5$–0.7, are presented in Fig. 8 (solid line). No clear characteristic of phase transition can be observed for all the samples in the testing temperature range. In general, the temperature-independent α (corresponding to a linear thermal expansion) or weakly temperature-dependence α is expected in pure paraelectric states [38–40]. Burns temperature (T_B) is defined as the temperature at which remarkable deviation from such character of behavior begins. To separate the regular and anomalous contributions to the thermal expansion, two methods are usually used. Firstly, the general approach is to approximate $\Delta L/L(T)$ data at high temperatures ($T > T_m$) by a straight line [39,41]. However, this approximation is poorly defined, especially for some cases where deviations from the linear temperature-dependence $\Delta L/L(T)$ and variation of $\alpha(T)$ are detected. The parameter α should approach zero as the temperature decreases. The relation between α and heat capacity within the Debye model should also be considered. As weakly temperature-dependence α is expected in a cubic phase ($T > T_m \approx$ Debye temperature θ_D), and it is almost impossible to define θ_D by approximating the experimental data. The average value of $\theta_D \approx 432$ K is adopted [45]. And the data were approximated by the relation below [43].

$$\alpha_L(T) = aT + bC_D(T), \tag{4}$$

where $C_D(T)$ is Debye model heat capacity, θ_D is Debye temperature, t is the vibration frequency.

$$C_D(T) = 9R\left(\frac{\theta_D}{T}\right)^3 \int_0^{\theta_D/T} t^4 \frac{\exp(t)}{[\exp(t)-1]^2} dt. \tag{5}$$

Fig. 8(a) and (b) (dot line) indicate that the fitting is suitable in our case. Values of θ_D were about 187 °C, 157 °C and 248 °C for $x = 0.5$, 0.6

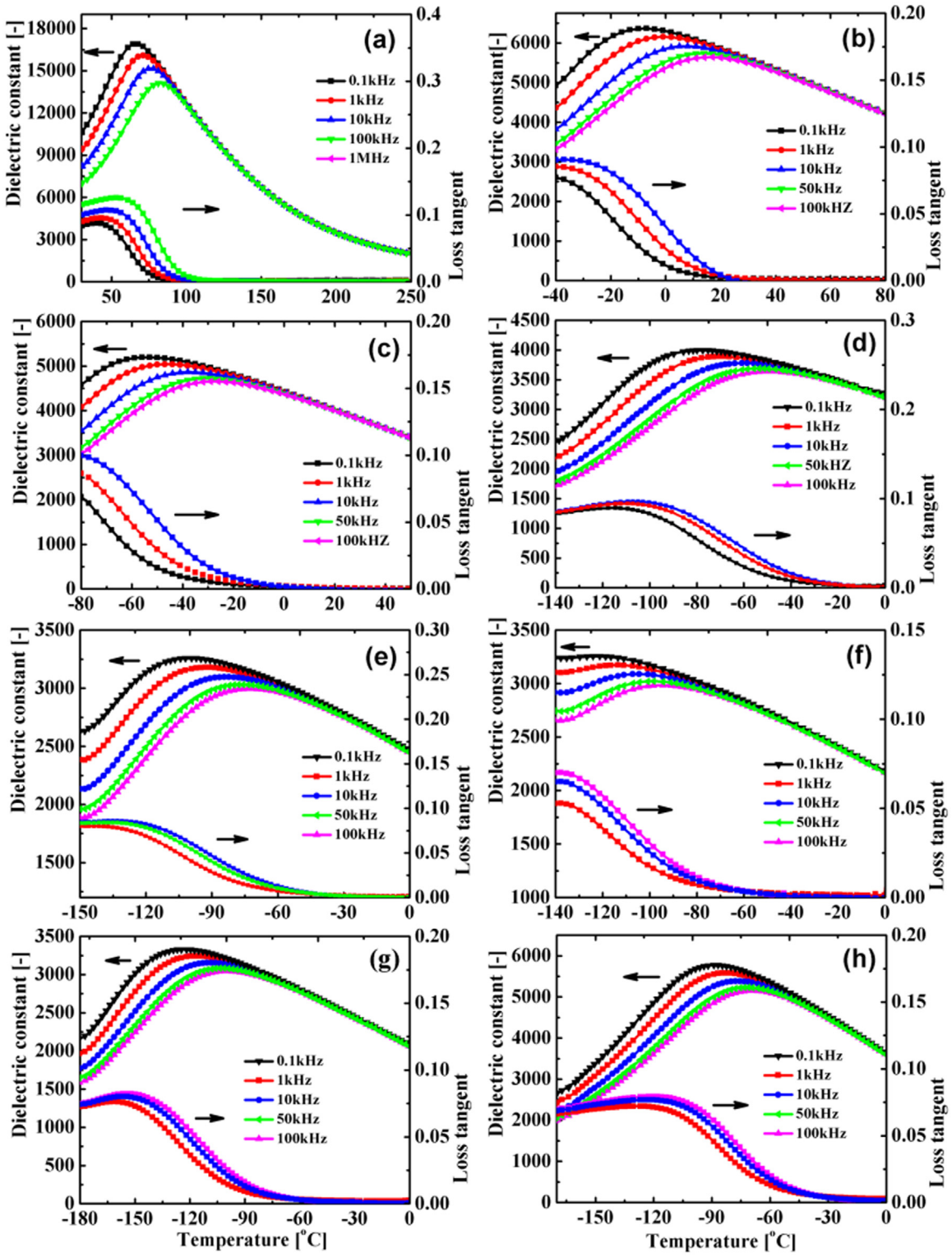

Fig. 3. The dielectric constant and loss tangent as a function of temperature measured at 0.1, 1, 10, 50 and 100 kHzfor $(1-x)$PZN-xBT ceramic samples with $x = 0.1$–0.8, corresponding to (a)–(h).

and 0.7 samples. Temperature dependence of anomalous $\Delta\alpha$ and $\Delta(\Delta L/L)$, for samples with $x = 0.5$–0.7, are shown in Fig. 9(a) and (b). The depletion point T_B can be estimated from temperature dependency of anomalous strain. And T_m can be defined from anomalous $\Delta\alpha(T)$. At the temperature blow T_B, temperature dependence of $\Delta L/L$ deviates from linear behavior (characteristic of high temperature), which is considered as the onset of polar nanoregions (PNRs). Moreover, the deviation of strain from classical theory also comes from the local electrostriction effect of PNRs [42,44]. For all the compositions, $T_B \approx 130 \pm 50\,^{\circ}\mathrm{C}$, $T_{max} \approx 270\,\mathrm{K}$ for $x = 0.5$, and $T_{max} \approx 220\,\mathrm{K}$ for $x = 0.6$. As for the $x = 0.7$ sample, it is difficult to define the position of T_m. In spite of their composition difference, samples ($x = 0.5$–0.7) possess similar T_B value. This kind of composition independence of T_B value have been reported in other BT-based solid solutions, such as

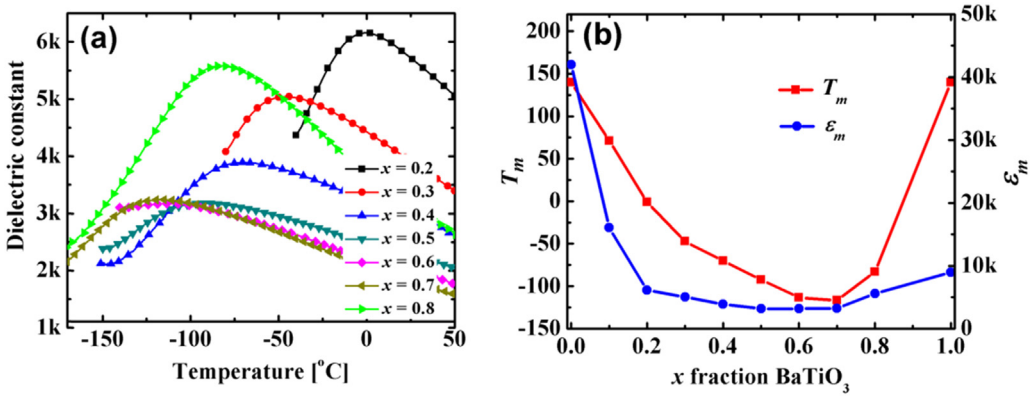

Fig. 4. Variation of dielectric constant (1 kHz) with temperature in the (a) for (1–*x*)PZN-*x*BT compositions, $x = 0.2$–0.8. T_m and ε_m vs. composition in the (b) for (1–*x*) PZN-*x*BT, $x = 0.1$–0.8, at 1 kHz, where the data for pure PZN and BT are from Ref. [28].

$BaTiO_3$-$BiSnO_3$, $BaTiO_3$-$BiScO_3$ [44,45].

Ferroelectric *P-E* hysteresis loops measured at room temperature and 1 Hz for $(1-x)$PZN-*x*BT are shown in Fig. 10(a) and (b). The slim hysteresis loop, which is a typical feature of relaxor ferroelectrics, can be observed. Note that, only in the composition with $x = 0.1$, the *P-E* hysteresis loop shows a tendency towards saturation at a relatively low field (~ 20 kV/cm). To better interpret the *P-E* hysteresis loops, *I-E* loops of representative PZN-BT ceramics are provided and shown in Fig. 10(c). The current peak corresponding to domain switching can be clear seen in the *I-E* loop of 0.9PZN-0.1BT ceramic. As the BT content increases, the current peak becomes weaker and weaker and cannot be observed in the *I-E* loop of 0.4PZN-0.6BT ceramic. However, the current peak appears again in 0.2PZN-0.8BT ceramic, although the peak is not that clear and sharp. As discussed in Yan et al.'s work, the current has contributions from the dielectric permittivity and domain switching. Thus, the variation of *I-E* loops can also describe the change of domains structures (or polar regions) in the PZN-BT system [46,47]. Fig. 10(d) shows the P_r and E_c as a function of the BT content summarized at room temperature and at 1 Hz. With the increasing BT contents, the P_r and E_c also change in the form of "U" curve. This phenomenon may be related to the variation of ΔT_m, which is used to characterize the degree of frequency dispersion, as shown in Fig. 7(b). It is reasonable to infer that the variation of hysteresis behavior derives from the disorder in the structure due to the substitution of the Ba^{2+} by Pb^{2+} and Ti^{4+} by Zn^{2+} and Nb^{5+}.

Table 1
The value of γ obtained from the fit to the Eq. (1) for $(1-x)$PZN-*x*BT system.

x	0.1	0.2	0.3	0.4	0.5	0.6	0.7	0.8
γ	1.81	1.64	1.89	1.65	1.79	1.82	1.71	1.83

In general, the PZN-BT ceramics show interesting dielectric relaxation and phase transition behaviors, where the T_m, P_r, and E_c change in the form of a "U" shaped curve with the increasing BT contents. As is known, the ferroelectricity of PZN mainly comes from the ordering of electronic and ionic coupling between A-site and O-site (A-O coupling), while that of BT mainly comes from the B-O coupling [48,49]. As BT is introduced to PZN, the A-O ordering may be disrupted by the A-site Ba^{2+} ions doping, leading to the decreased T_m. On the other hand, the B-O ordering is also affected by the B-site zinc and niobium ions doping. Thus, neither A-O ordering nor B-O ordering can be established in the intermediate compositions. Or in another words, the polarization mismatch happens. This explanation on the relaxation behaviors has similarity with the previous concept "nano phase separation" proposed in the same material system by Wang et al. [32,33]. The main difference is that the fluctuation of polarization and

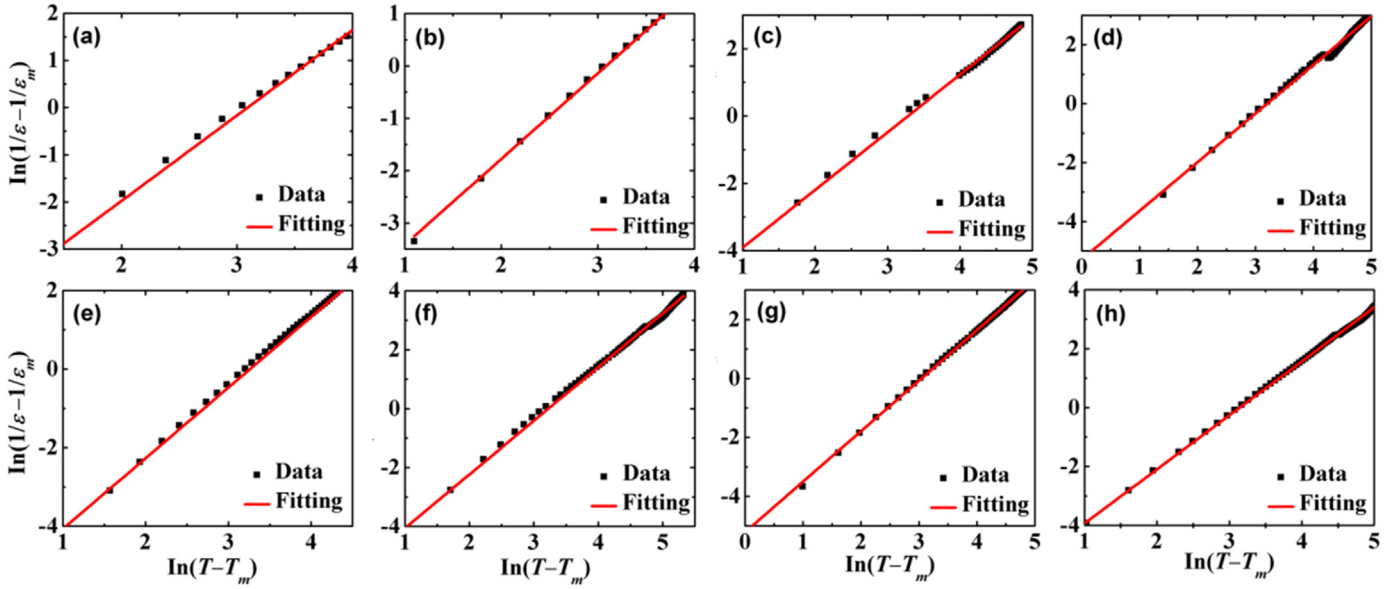

Fig. 5. (Dot lines) Processed dielectric constant $[\ln(1/\varepsilon - 1/\varepsilon_m)]$ as a function of logarithm of temperature $[\ln(T - T_m)]$ at 1 kHz for $(1-x)$PZN-*x*BT, where $x = 0.1$–0.8, corresponding to (a)–(h). Solid lines are the fittings to the Eq. (1), for $(1-x)$PZN-*x*BT: $x = 0.1$–0.8, corresponding to (a)–(h).

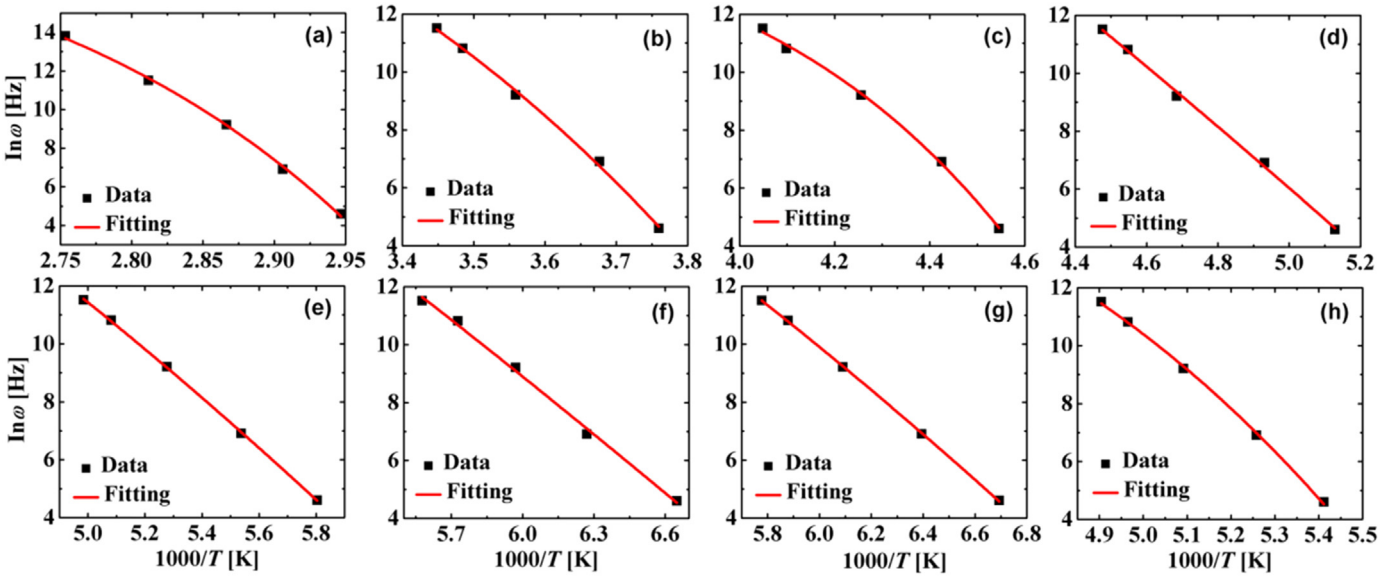

Fig. 6. (Scatter dots) Logarithm of frequency (lnω) as a function of reciprocal of temperature ($1/T$) for $(1-x)$PZN-xBT, where x = 0.1–0.8, corresponding to (a)–(h). Solid lines are the fittings to the Eq. (2), for $(1-x)$PZN-xBT ceramic samples with x = 0.1–0.8, corresponding to (a)–(h).

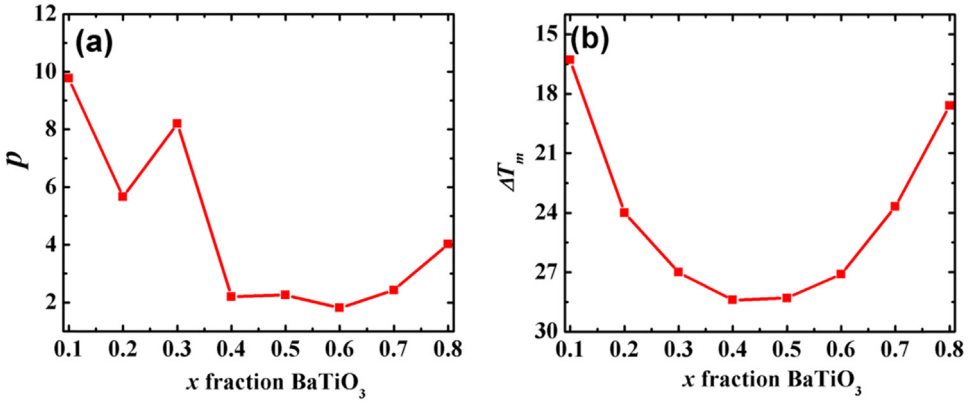

Fig. 7. Variation of p in the (a) and ΔT_m, where $\Delta T_m = \Delta T_{m\ (100kHz)} - \Delta T_{m\ (100Hz)}$, in the (b) vs. composition in PZN-BT system.

Table 2
P, E_a and ω_0 obtained from the fit to the new glass model for $(1-x)$PZN-xBT system.

x	0.1	0.2	0.3	0.4	0.5	0.6	0.7	0.8
p	9.77	5.66	8.20	2.20	2.26	1.81	2.43	4.03
E_a (eV)	0.31	0.238	0.0427	0.14	0.11	0.11	0.12	0.076
ω_0 (Hz)	1.79×10^{10}	4.6×10^{9}	6.3×10^{6}	2.9×10^{13}	2.4×10^{12}	1.9×10^{13}	1.9×10^{12}	1.5×10^{11}

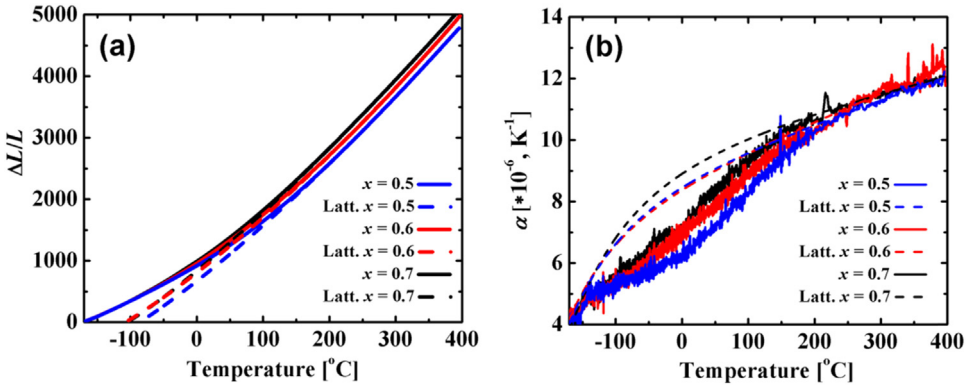

Fig. 8. Temperature dependence of thermal expansion coefficient α (a) and strain $\Delta L/L$ (b) for (1-x)PZN-xBT ceramics, ($0.5 \le x \le 0.7$). Solid lines are experimental data and dot lines are approximated by Eq. (4).

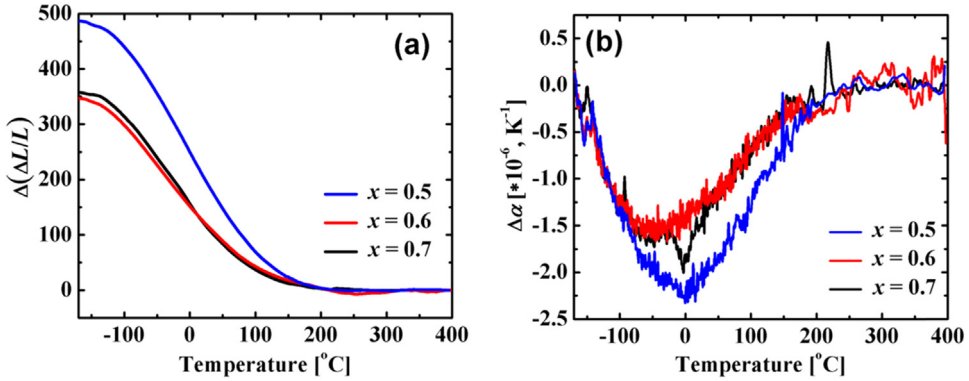

Fig. 9. Temperature dependence of anomalous thermal expansion coefficient $\Delta\alpha$ in the (a) and strain $\Delta L/L$ in the (b) for (1-x)PZN-xBT ceramics, ($0.5 \le x \le 0.7$).

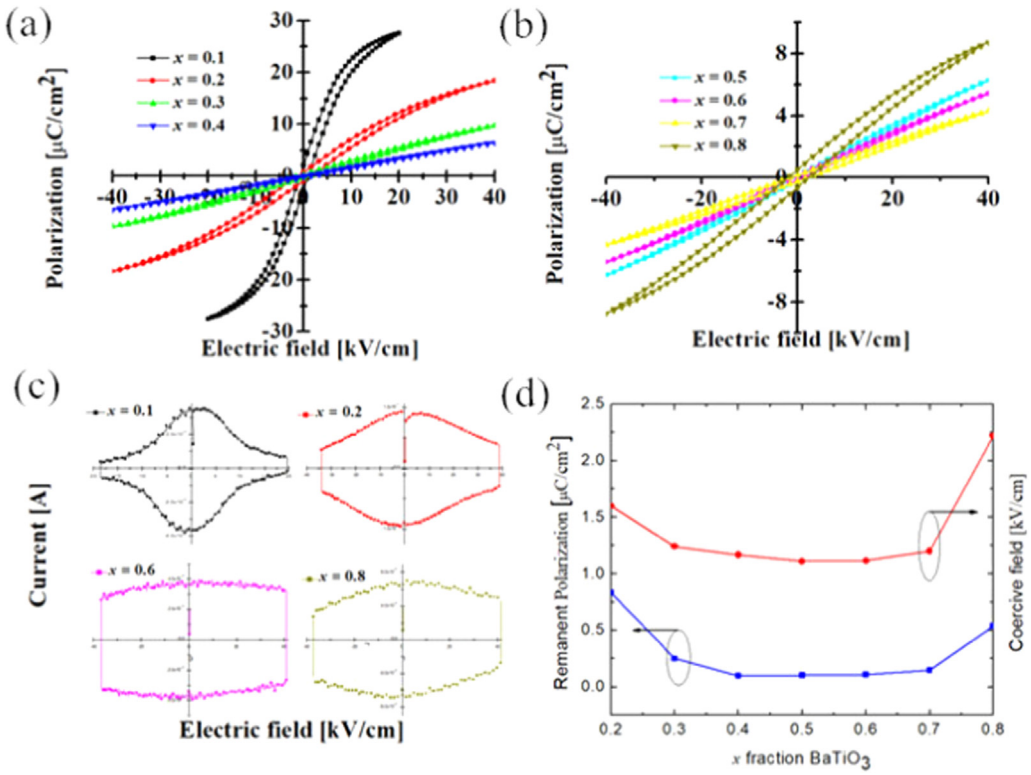

Fig. 10. (a) and (b) *P-E* hysteresis loops of PZN-BT ceramics measured at ambient temperature with a triangular wave form at 1 Hz. (c) *I-E* loops of representative PZN-BT ceramics (d) the remnant polarization (P_r) and coercive field (E_c) summarized at room temperature and 1 Hz as a function of BT content for (1-x)PZN-xBT ceramics, ($0.2 \le x \le 0.8$).

ferroelectric order, rather than chemical composition, is emphasized here. The polarization mismatches frustrate the long range ferroelectric order by cross occupying in both A-site and B-sites. On microscopic scale, local regions at nanometer scale fluctuate in composition and consequently, in polarization. This structural feature leads to peculiar characteristics, such as low T_m, broadened dielectric peak and slim hysteresis loop. Similar phenomena can also be observed in bismuth based solid solution systems, including BMT-BT [20,21], BMN-BT [24] and BS-BT [18,19]. The common features of these material systems may also arise from polarization mismatches. A sharp contrast can be observed for the above materials systems if replace BT with PT, where normal ferroelectric such as PMN-PT and PZN-PT, BF-PT, BS-PT appear. The disappearance of the"U"shape curve is due to the A-O coupling in PT where polarization mismatches cannot be established. This phenomenon also proves our theory of polarization mismatches.

In fact, there are also other mechanisms that explain the enhancement of the relaxor properties when Pb^{2+} is replaced by Ba^{2+} reported by many researchers [50–53]. Generally, these literatures focus on the effect of Ba^{2+} on the destruction of the long range order structure in ferroelectric ceramics. With the increasing Ba^{2+} concentration, transition from normal ferroelectric phase to relaxor ferroelectric phase and paraelectric phase is shown in the $Pb_{(1-x)}Bax(Mg_{1/3}Nb_{2/3})_m(Zn_{1/3}Nb_{2/3})_y(Ni_{1/3}Nb_{2/3})_nTi_zO_3$($x$ = 0–0.15,m,n,y) ceramics. In the PZN-BT system discussed in this paper, such variation can also be obtained in compositions with BT content lower than 0.6. While, the re-establishment of the long range order is visualized when higher BT is added, which is not discussed in these literatures. Actually, the proposed polarization mismatched model stress on the destruction of long range order caused by the ionic substitutions on A- and B- site of the perovskite structure. As far as we know, solid solutions with such a polarization mismatched behavior are quite common, while explicit explanations are not given yet.

4. Conclusions

In this work, the composition dependence of the properties of (1–x) PZN-xBT solid solutions (x = 0.1–0.8), including the dielectric constant and loss tangent, thermal expansion coefficient, and *P-E* hysteresis loops were studied systematically. The ε_m, T_m, p, P_r, and E_c all change in form of "U" shape curves with respect to the increasing BT contents.

Normal B-O coupling ferroelectric BT is doped into the A-O coupling relaxor ferroelectric PZN, leading to an existing relaxor ferroelectric (1–*x*)PZN-*x*BT with complex local coupling conditions. A polarization mismatch model is proposed to illustrate the underlying mechanism, which ascribes the "U" shape curve to the frustration and re-establishment of polarization.

Acknowledgments

This work was supported by the National Basic Research Program of China (Grant No. 2015CB654602), the International Science & Technology Cooperation Program of China (Grant No. 2015DFA51100), the NSFC projects (Grant Nos. 51761145024 and 51772239), Shaanxi province project 2017 ktpt-21, the Joint fund of the Ministry of Education (Grant No. 6141A02033210) and the 111 Project under Grant No. B14040. The SEM work was done at International Center for Dielectric Research (ICDR), Xi'an Jiaotong University, Xi'an, China.

References

[1] G.A. Samara, The relaxational properties of compositionally disordered ABO_3 perovskites, J. Phys.: Condens. Matter 15 (2003) 367–411.
[2] V.V. Shvartsman, D.C. Lupascu, Lead-free relaxor ferroelectrics, J. Am. Ceram. Soc. 95 (2012) 1–26.
[3] R.A. Cowley, S.N. Gvasaliya, S.G. Lushnikov, B. Roessli, G.M. Rotaru, Relaxing with relaxors: a review of relaxor ferroelectrics, Adv. Phys. 60 (2011) 229–327.
[4] G.A. Smolenskii, V.A. Isupov, Segnetoelektricheskie svoistva tverdykh rastvorov stannata bariya v titanate bariya, Zh. Tekh. Fiz. 24 (1954) 1375–1386.
[5] Q. Hu, L. Jin, T. Wang, C. Li, Z. Xing, X. Wei, Dielectric and temperature stable energy storage properties of $0.88BaTiO_3$-$0.12Bi(Mg_{1/2}Ti_{1/2})O_3$ bulk ceramics, J. Alloy. Compd. 640 (2015) 416–420.
[6] Q. Hu, T. Wang, L. Zhao, L. Jin, Z. Xu, X. Wei, Dielectric and energy storage properties of $BaTiO_3$-$Bi(Mg_{1/2}Ti_{1/2})O_3$ ceramic: influence of glass addition and biasing electric field, Ceram. Int. 43 (2017) 35–39.
[7] L. Jin, F. Li, S. Zhang, Decoding the fingerprint of ferroelectric loops: comprehension of the material properties and structure, J. Am. Ceram. Soc. 97 (2014) 1–27.
[8] L. Jin, R. Huo, R. Guo, F. Li, D. Wang, Y. Tian, Q. Hu, X. Wei, Z. He, Y. Yan, G. Liu, Diffuse phase transitions and giant electrostrictive coefficients in lead-free Fe^{3+}-doped $0.5Ba(Zr_{0.2}Ti_{0.8})O_3$-$0.5(Ba_{0.7}Ca_{0.3})TiO_3$ ferroelectric ceramics, ACS Appl. Mater. Interfaces 8 (2016) 31109–311119.
[9] Y. Tian, L. Jin, H. Zhang, Z. Xu, X. Wei, E.D. Politova, S.Y. Stefanovich, N.V. Tarakina, I. Abrahams, H. Yan, High energy density in silver niobate ceramics, J. Mater. Chem. A 4 (2016) 17279–17287.
[10] A. Kumar, I. Rivera, R.S. Katiyar, Investigation of local structure of lead-free relaxor $Ba(Ti_{0.70}Sn_{0.30})O_3$ by Raman spectroscopy, J. Raman Spectrosc. 40 (2009) 459–462.
[11] J. Ravez, A. Simon, Some solid state chemistry aspects of lead-free relaxor ferroelectrics, J. Solid State Chem. 162 (2001) 260–265.
[12] G. Burns, F.H. Dacol, Glassy polarization behavior in ferroelectric compounds $Pb(Mg_{1/3}Nb_{2/3})O_3$ and $Pb(Zn_{1/3}Nb_{2/3})O_3$, Solid State Commun. 48 (1983) 853–856.
[13] V. Westphal, W. Kleemann, M. Glinchuk, Diffuse phase transitions and random-field-induced domain states of the "relaxor" ferroelectric $PbMg_{1/3}Nb_{2/3}O_3$, Phys. Rev. Lett. 68 (1992) 847–850.
[14] A.A. Bokov, Z.-G. Ye, Recent progress in relaxor ferroelectrics with perovskite structure, J. Mater. Sci. 41 (2006) 31–52.
[15] B.E. Vugmeister, Polarization dynamics and formation of polar nanoregions in relaxor ferroelectrics, Phys. Rev. B 73 (2006) 174117.
[16] B.P. Burton, E. Cockayne, U.V. Waghmare, Correlations between nanoscale chemical and polar order in relaxor ferroelectrics and the lengthscale for nanoregions, Phys. Rev. B 72 (2005) 064113.
[17] G. Xu, G. Shirane, J.R.D. Copley, P.M. Gehring, Neutron elastic diffuse scattering study of $PbMg_{1/3}Nb_{2/3}O_3$, Phys. Rev. B 69 (2004) 064112.
[18] F. Chu, I.M. Reaney, N. Setter, Spontaneous (zero-field) relaxorto-ferroelectric-phase transition in disordered $Pb(Sc_{1/2}Nb_{1/2})O_3$, J. Appl. Phys. 77 (1995) 1671–1676.
[19] A.A. Bokov, Z.-G. Ye, Recent progress in relaxor ferroelectrics with perovskite structure, J. Mater. Sci. 41 (2006) 31–52.
[20] M. Yoshida, S. Mori, N. Yamamoto, Y. Uesu, J.M. Kiat, TEM observation of polar domains in relaxor ferroelectric $Pb(Mg_{1/3}Nb_{2/3})O_3$, Ferroelectrics 217 (1998) 327–333.
[21] A. Zeb, S.J. Milne, Temperature-stable dielectric properties from − 20 °C to 430 °C in the system $BaTiO_3$-$Bi(Mg_{0.5}Zr_{0.5})O_3$, J. Eur. Ceram. Soc. 34 (2014) 3159–3166.
[22] T. Wang, L. Jin, C. Li, Q. Hu, X. Wei, Relaxor ferroelectric $BaTiO_3$–$Bi(Mg_{2/3}Nb_{1/3})O_3$ ceramics for energy storage application, J. Am. Ceram. Soc. 98 (2015) 559–566.
[23] D. Kwon, M.H. Lee, Temperature-stable high-energy-density capacitors using complex perovskite thin films, IEEE Trans. Ultrason. Eng. 59 (2012) 1894–1899.
[24] D.H. Choi, A. Baker, M. Lanagan, S. Trolier-McKinstry, C. Randall, Structural and dielectric properties in $(1-x)BaTiO_3$–$xBi(Mg_{1/2}Ti_{1/2})O_3$ ceramics ($0.1 \le x \le 0.5$) and potential for high-voltage multilayer capacitors, J. Am. Ceram. Soc. 96 (2013) 2197–2202.
[25] Z. Li, Z. Li, Q. Li, L. Zhang, X. Yao, Dielectric properties and transition temperature of ceramics in the $Pb(Mn_{1/3}Nb_{2/3})O_3$–$BaTiO_3$ system, Ferroelectrics 262 (2001) 1021–1026.
[26] T. Wang, L. Jin, Y. Tian, L. Shu, Q. Hu, X. Wei, Microstructure and ferroelectric properties of Nb_2O_5-modified $BiFeO_3$-$BaTiO_3$ lead free ceramics for energy storage, Mater. Lett. 137 (2014) 79–81.
[27] Y. Yokomizo, T. Takahashi, S. Nomura, Ferroelectric properties of $Pb(Zn_{1/3}Nb_{2/3})O_3$, J. Phys. Soc. Jpn. 28 (1970) 1278–1284.
[28] J. Kuwata, K. Uchino, S. Nomura, Diffuse phase transition in lead zinc niobate, Ferroelectrics 22 (1978) (1978) 863–867.
[29] H. Arvind, K. Umesh, R.E. Newnham, L.E. Cross, Stabilization of the perovskite phase and dielectric properties of ceramics in the $Pb(Zn_{1/3}Nb_{2/3})O_3$-$BaTiO_3$ system, Am. Ceram. Soc. Bull. 66 (1987) 671–676.
[30] J.R. Belsick, A. Halliyal, U. Kumar, R.E. Newnham, Phase relations and dielectric properties of ceramics in the system $Pb(Zn_{1/3}Nb_{2/3})O_3$-$PbTiO_3$-$SrTiO_3$, Am. Ceram. Soc. Bull. 66 (1987) 664–667.
[31] S.E. Park, T.R. Shrout, Ultrahigh strain and piezoelectric behavior in relaxor based ferroelectric single crystal, J. Appl. Phys. 82 (1997) 1804–1811.
[32] D.H. Lee, N.K. Kim, Crystallographic, dielectric and diffuseness characteristics of PZN-PT ceramics, Mater. Lett. 34 (1998) 299–304.
[33] V.A. Isupov, Causes phenomena transition broadening and nature of dielectric polarization relaxation in some ferroelectrics, Sov. Phys. Solid State 5 (1963) 136–140.
[34] G.A. Smolenskii, Physical phenomena in ferroelectrics with diffused phase transition, J. Phys. Soc. Jpn. 28 (1970) 26–37.
[35] Z.Y. Cheng, L.Y. Zhang, X. Yao, Investigation of glassy behaviour of lead magnesium niobate relaxors, J. Appl. Phys. 79 (1996) 8615–8619.
[36] D. Viehland, The Glassy Behavior of Realxor ferroelectrics [D] (Ph.D. Thesis), The Pennsylvania State University, 1992.
[37] C.C. Huang, D.P. Cann, X. Tan, N. Vittayakorn, Phase transitions and ferroelectric properties in $BiScO_3$-$Bi(Zn_{1/2}Ti_{1/2})O_3$-$BaTiO_3$ solid solution, J. Appl. Phys. 102 (2007) 044103.
[38] S. Anwar, P.R. Sagdeo, N.P. Lalla, Ferroelectrics relaxor behavior in hafnium doped barium-titanate ceramic, Solid State Commun. 138 (2006) 331–336.
[39] H. Arndt, G. Schmidt, Thermal expansion in relaxor ferroelectric, Ferroelectrics 79 (1998) 443–446.
[40] A.S. Bhalla, R. Guo, L.E. Cross, Measurements of strain and the optical indices in the ferroelectric $Ba_{0.4}Sr_{0.6}Nb_2O_6$: polarization effects, Phys. Rev. B 36 (1987) 2030–2035.
[41] M.V. Gorev, I.N. Flerov, P. Sciau, V.S. Bondarev, A. Geddo-Lehmann, Heat capacity and thermal expansion studies of relaxors, Ferroelectrics 307 (2004) 127–136.
[42] G. Burns, F.H. Dacol, Crystalline ferroelectrics with glassy polarization behavior, Phys. Rev. B 28 (1983) 2527–2530.
[43] W.N. Lawless, Debye temperature of ferroelectrics, Phys. Rev. B 17 (1978) 1458–1459.
[44] M. Gorev, V. Bondarev, I. Flerov, M. Maglione, A. Simon, P. Sciau, M. Boulos, S. Guillemet-Fritsch, Thermal expansion, polarization and phase diagrams of $Ba_{1-y}Bi_{2y/3}Ti_{1-x}Zr_xO_3$ and $Ba_{1-y}LayTi_{1-y/4}O_3$ compouds, J. Phys.: Condens. Matter 21 (2009) 075902.
[45] C. Lei, A.A. Bokov, Z.-G. Ye, Ferroelectric to relaxor crossover and dielectric phase diagram in the $BaTiO_3$-$BaSnO_3$ system, J. Appl. Phys. 101 (2007) 084105.
[46] H. Yan, F. Inam, G. Viola, H. Ning, H. Zhang, Q. Jiang, T. Zeng, Z. Gao, M.J. Reece, The contribution of electrical conductivity, dielectric permittivity and domain switching in ferroelectric hysteresis loops, J. Adv. Dielectr. 1 (2011) 107–118.
[47] J. Wu, A. Mahajan, L. Riekehr, H. Zhang, B. Yang, N. Meng, Z. Zhang, H. Yan, Perovskite $Srx(Bi_{1-x}Na_{0.97-x}Li_{0.03})_{0.5}TiO_3$ ceramics with polar nano regions for high power energy storage, Nano Energy 50 (2018) 723–732.
[48] H. Yu, Z.-G. Ye, Dielectic properties and relaxor behavior of a new $(1-x)BaTiO_3$-$xBiAlO_3$ solid solution, J. Appl. Phys. 103 (2008) 034114.
[49] R.E. Cohen, H. Krakauer, Lattice dynamics and orgin of ferroelectricity in $BaTiO_3$: linearized-augmented-plane-wave total-energy calculations, Phys. Rev. B 42 (1990) 6416–6423.
[50] R.A. Cowly, S.N. Gvasaliya, S.G. Lushnikov, B. Roessli, G.M. Rotaru, Relaxing with relaxors: a review of relaxor ferroelectircs, Adv. Phys. 60 (2001) 229–327.
[51] B.-Y. Ahn, N.-K. Kim, Effects of barium substitution on perovskite formation, dielectric properties, and diffuseness characteristics of lead zinc niobate ceramics, J. Am. Ceram. Soc. 83 (2000) 1720–1726.
[52] V. Marinova, B. Mihailova, T. Malcherek, C. Paulmann, K. Lengyel, L. Kovacs, M. Veleva, M. Gospodinov, B. Guttler, R. Stosch, U. Bismayer, Structural, optical and dielectric properties of relaxor-ferroelectric $Pb_{0.78}Ba_{0.22}Sc_{0.5}Ta_{0.5}O_3$, J. Phys.: Condens. Matter 18 (2006) 075902.
[53] M.V. Talanov, L.A. Shilkina, I.A. Verbenko, L.A. Reznichenko, Impact of Ba^{2+} on structure and piezoelectric properties of PMN–PZN–PNN–PT ceramics near the morphotropic phase boundary, J. Am. Ceram. Soc. 98 (2015) 838–847.